



OPEN

Intercellular interactions between mast cells and stromal fibroblasts obtained from canine cutaneous mast cell tumours

Lidia H. Pulz^{1,2}, Yonara G. Cordeiro², Greice C. Huete², Karine G. Cadrobbi², Arina L. Rochetti², Pedro L. P. Xavier², Adriana Tomoko Nishiyama³, Silvio Henrique de Freitas², Heidge Fukumasu² & Ricardo F. Strefezzi²✉

Mast cell tumours (MCTs) are the most frequent malignant skin neoplasm in dogs. Due to the difficulty in purifying large numbers of canine neoplastic mast cells, relatively little is known about their properties. A reproducible *in vitro* model is needed to increase the understanding about the phenotype and functional properties of neoplastic mast cells. In the present study, we describe the establishment of primary cocultures of neoplastic mast cells from canine cutaneous MCTs and cancer-associated fibroblasts. We confirmed the inability of canine neoplastic mast cells to remain viable for long periods *in vitro* without the addition of growth factors or *in vivo* passages in mice. Using a transwell system, we observed that mast cell viability was significantly higher when there is cell-to-cell contact in comparison to non-physical contact conditions and that mast cell viability was significantly higher in high-grade than in low-grade derived primary cultures. Moreover, the use of conditioned medium from co-cultured cells led to a significantly higher tumoral mast cell viability when in monoculture. Signalling mechanisms involved in these interactions might be attractive therapeutic targets to block canine MCT progression and deserve more in-depth investigations.

Mast cells play an important role in the pathogenesis of inflammatory and allergic reactions¹, but neoplastic proliferation can severely affect the dog skin. Mast cell tumours (MCTs) represent 11–27% of all malignant skin neoplasms in this species and the treatment is considered challenging due to the highly variable behaviour of the tumour². Due to the difficulty in reliably purifying large numbers of canine neoplastic mast cells, relatively little is known about their properties. Previous investigations using non-neoplastic mast cells in short-term cultures have contributed to our understanding of phenotypic and functional features^{3–7}, but a reproducible *in vitro* model that employs canine neoplastic mast cells and stromal malignant counterparts should be considered as an effective tool to study the canine mast cell tumour at the cellular and molecular levels.

One of the main reasons for the failure to establish primary cell-cultures from canine MCTs has been the difficulty in isolating and maintaining viable primary cells from the solid neoplastic masses. Most of the studies performed with canine neoplastic mast cell lines in permanent culture were obtained from freshly disaggregated MCTs that were subsequently inoculated in athymic/nude^{8–11} or severe combined immunodeficiency (SCID) mice¹². Although a great amount of useful data has been generated, the limitation is obvious: malignant mast cells are influenced by the mouse microenvironment. Canine bone marrow-derived mast cells (BMMCs) were also used for *in vitro* studies⁷ but several important differences were demonstrated between immature BMMCs and mature mast cells through transcriptome analysis¹³, which can limit the relevance of this model.

The process of generating mast cells *in vitro* is species-specific⁷, suggesting that certain aspects of canine mast cell biology cannot be established with human mast cells. Therefore, *in vitro* models are needed to reflect MCT biology *in vivo* more accurately and to enable long-term studies. Human connective tissue mast cells were successfully maintained *ex vivo* with skin-derived fibroblasts for up to 13 days¹⁴. Additional coculture studies performed with mouse mast cells and fibroblasts showed that the mast cell phenotype is profoundly influenced by

¹Faculdade de Medicina Veterinária e Zootecnia, Universidade de São Paulo, Av. Prof. Dr. Orlando Marques de Paiva, 87, São Paulo, SP CEP 05508-270, Brazil. ²Laboratório de Oncologia Comparada e Translacional, Faculdade de Zootecnia e Engenharia de Alimentos, Universidade de São Paulo, Campus "Fernando Costa", Av. Duque de Caxias Norte 225, Pirassununga, SP CEP 13635-900, Brazil. ³Hospital Veterinário da Universidade Anhembi Morumbi, R. Conselheiro Lafaiete, 64, São Paulo, SP CEP 03101-00, Brazil. ✉email: rstrefezzi@usp.br

interactions with fibroblast products^{15,16}, promoting differentiation in BMMCs¹⁷, as well as maturation modulated by fibroblasts¹⁸. On the other hand, mast cells were also able to stimulate stroma modulation through the release of potent fibrogenic substances and induction of matrix metalloproteinases (MMPs) release from fibroblasts when in cell-to-cell contact^{19–21}.

Considering the context of solid cancers, several studies have focused on coculture techniques to explore the cancer-mediated regulation by cancer-associated fibroblasts (CAFs) but none of them are exclusive to canine tumours^{22–27}. Recently, CAFs were demonstrated to be immersed in MCT stroma^{28,29} but canine neoplastic mast cell interactions with the extracellular microenvironment have not been widely investigated.

In this paper, we describe the establishment of primary co-cultures of neoplastic mast cells and cancer associated fibroblasts (CAFs) from canine cutaneous MCTs and explore the relationship of both cell types by coculture experiments in which cancer cells and fibroblasts were separated by a transwell chamber with micropores that allowed cell-to-cell communication through soluble factors.

Results

Study population. Fourteen MCT samples were obtained from twelve dogs immediately after the excisional biopsy. Thirteen were used for cell viability assays and one sample (401–18) was available only for the coculture assays. The age of the dogs ranged from 3 to 14 years (mean = 7.6 years old). Females (58.3%) were more frequent than males (41.7%). Considering the breed distribution, 41.7% (5/12) of the MCTs cases were mongrel dogs and 58.3% (7/12) were purebred dogs. Seven tumours (50%) were high-grade MCTs and 7 (50%) were low-grade³⁰. The characteristics of the dog population and histological classifications of each lesion are described in Table S1 (Supplementary materials).

Culture characterization of canine MCT. To observe the natural course of primary canine MCT cells *in vitro*, we harvested thirteen samples from eleven dogs (samples 1–13) immediately after the excisional biopsy, and monitored cell progression for up to 11 weeks by phase contrast microscope imaging analyses and cell viability measurement. Next, we demonstrated that all canine MCT primary cultures were composed by two major cell types: non-adherent cells (mast cells) and adherent cells (fibroblast-like) (Fig. 1). The vast majority of neoplastic mast cells ceased to proliferate and begun to die under *in vitro* conditions. Adherent cells after the initial seeding were identified as fibroblast-like with progressive proliferation. In all tumour samples, adherent cells rapidly multiplied to form a confluent monolayer under the neoplastic mast cells in 7–14 days (Fig. 1).

During all the passages of the primary culture, neoplastic mast cells were non-adherent cells isolated or forming floating aggregates. Mast cell population was maintained in clumps in continuity with the adherent layer with fibroblastic characteristics. At the beginning of the study and in each passage, neoplastic mast cells were characterized using Toluidine blue and Romanowsky stains to visualize the distinguished morphological features as the round-shaped cytoplasm, round to oval uniform-sized nuclei and variable quantities of metachromatic granules typical of cultured mast cells (Fig. 2). It was noted that these cells were progressively losing their granules in the culture over time.

Phenotypic properties of adherent cells. We further analysed the phenotypes of the adherent cells differentiated into spindle-shape morphology. The success rate to generate fibroblastic-type cells in primary MCT cultures was 100%. Before distinguishing adherent cells in CAFs and non-cancer-associated fibroblasts (NCAFs), we characterized the fibroblast primary cultures by reverse transcription polymerase chain reaction (RT-PCR) using the Fibroblast-specific Protein 1 messenger RNA (FSP1 mRNA). Adherent cells from two tumour samples were evaluated on P0 and P1 and both displayed higher expression of this gene in comparison with canine cancer cells (M5 and M25) (Table 1; Fig. 3). We also characterized the other fibroblast primary cultures using RNA-seq data. Using global gene expression, we observed a strong cluster difference between fibroblasts and canine cancer cells (Supplementary Figs. S1 and S2). In addition, differential gene expression analysis showed that fibroblast-associated genes FSP1 and FAP are upregulated in fibroblast primary cultures in comparison with canine cancer cells lines (Table 2).

Comparisons were performed between canine cancer cells (M5 and M25) and adherent fibroblasts (H250, H346, H395, H401, H402 and H1171). Canine cancer cells were used as reference samples to logFold-Change (logFC) analysis. Both FSP1 and FAP genes are significantly upregulated in fibroblasts as shown by the logFC values.

Immunofluorescent staining of adherent cells with fibroblasts phenotype (a spindle, flattened-spindle, or less frequently triangular shape, with frequent long terminal threadlike processes) revealed myofibroblast features, including vimentin and α -SMA expression (Fig. 4).

Cell viability in primary cocultures. We evaluated cell viability of each MCT to determine the maintenance time of viable neoplastic mast cells *in vitro* cocultured with CAFs. Thus, non-adherent cells were stained with Trypan blue exclusion test to quantify the viable mast cells in the supernatant in each passage. Cultures were seeded with a total number of cells ranged from 5.5×10^5 to 3.6×10^6 cells/mL (mean $1.5 \times 10^6 \pm 1,034,832$). Neoplastic mast cells remained viable for a period that ranged from 30 to 75 days (average time of 57.7 days). In all samples, viable mast cells decreased during culture passage in number and percentage of cells (Fig. 5) which was consistent with the observed in the analysis of the different passages in the microscope. The number and percentage of viable mast cells obtained after digestion of skin MCT for each lesion and passage can be seen in Supplementary Tables S2 to S14 (Supplementary Materials).

In addition to cell viability, adherent cells were examined using beta-galactosidase (SA- β -Gal) activity assay. All samples in middle and late passage cultures (starting from P4), CAFs and NCAFs ceased to be confluent and

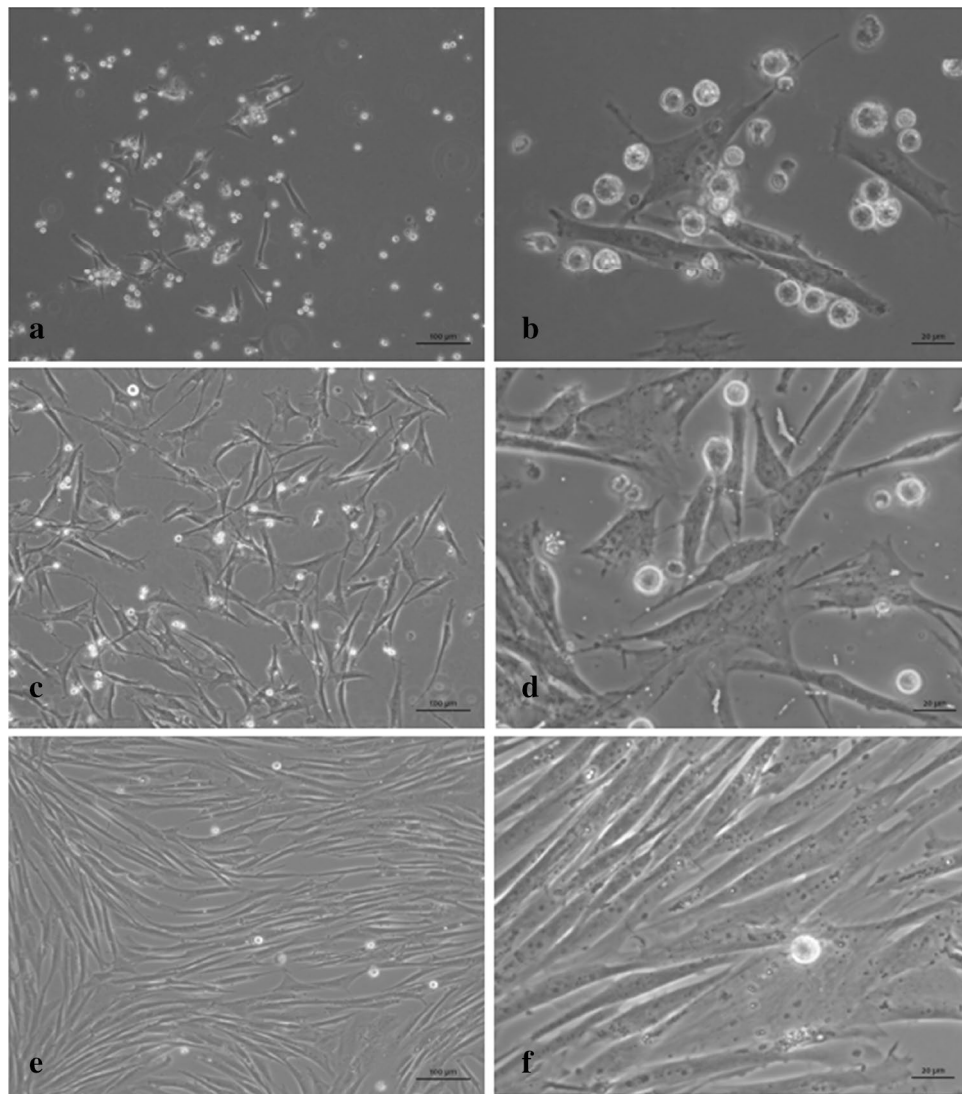


Figure 1. Microscopic features of canine MCT culture sample H334-16. **(a,b)** Early passage (P0) 4 days after initiation of culture, showing small clumps as well as individual neoplastic mast cells in the supernatant in association with the adherent layer. **(c,d)** 14 days of cultivation (P1 passage), with primary mast cells overlaying fibroblasts. **(e,f)** 34 days of cultivation, showing low number of viable mast cells in the supernatant and the fibroblasts tending to confluence. Phase contrast microscope. Bars = 100 µm **(a,c,e)** and 20 µm **(b,d,f)**.

begun to change their phenotype to an enlarged cell morphology with depleted replicative potential. Senescence-associated beta-galactosidase (SA- β -Gal) activity was measured in late passages, with several strongly positive cells for SA- β -Gal, mainly in perinuclear area (Fig. 6). Notably, passages showing a high number of SA- β -Gal-positive adherent cells presented loss of replicative capacity, revealed by failure to reach confluence.

Cocultures and transwell assay. Dissociated cells from canine MCTs, seeded and cultured for up to 48 h could be distinguished between two cell subpopulations: adherent (CAFs and NCAFs) and non-adherent (mast cells). To address the importance of stromal cells for neoplastic mast cells in vitro maintenance, we performed transwell experiments to observe physical and/or chemical effects of CAFs and NCAFs on the canine tumoral mast cells viability. Four co-culture conditions were tested: tumour mast cells and fibroblast direct cell-to-cell contact; tumour mast cells and fibroblast physically separated by the insert; tumour mast cells in monoculture supplemented with complete conditioned medium (CCM); and tumour mast cells in monoculture supplemented with basic medium consisting only of FBS and antibiotics (CDMEM-F12). Four dogs with single MCTs (two low-grade and two high-grade) were selected in these experiments to ensure we were dealing with primary tumours.

Thus, by using neoplastic adherent and mast cells from the same tumour, we observed that both time and culture condition contributed to variation in survival of co-cultured cells ($P < 0.01$). At all time-points, viability of neoplastic mast cells was significantly higher in the cell-to-cell contact condition compared to mast cell

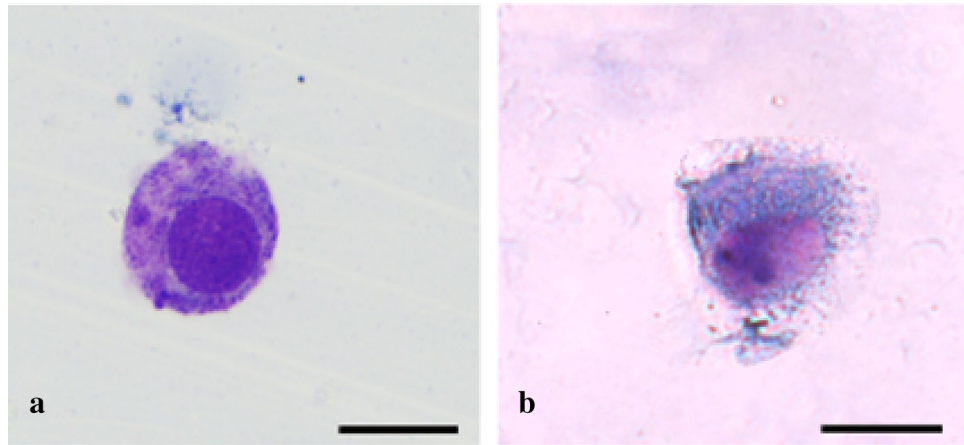


Figure 2. Mast cells 5 days after initiation of culture. (a) Romanowsky-stained preparation and (b) toluidine blue-stained preparation. Bars = 20 μm.

Sample	FSP1 Ct Mean	18S Ct Mean	2 ^{ΔΔCt} Mean
334–16 (P0)	32.61 ± 0.29	27.28 ± 0.08	93.92 ± 13.86
346–16 (P1)	23.77 ± 0.008	20.29 ± 0.19	338.46 ± 46.58
M5	23.06 ± 0.06	11.45 ± 0.02	1.20 ± 0.03
M25	23.24 ± 0.03	11.11 ± 0.007	0.83 ± 0.01

Table 1. FSP1 mRNA levels measured by real-time PCR and normalized by 18S ribosomal RNA (rRNA). Ct (cycle threshold) values to FSP1 and 18S of P0, P1, M5 and M25 cells are observed as mean ± Sd.

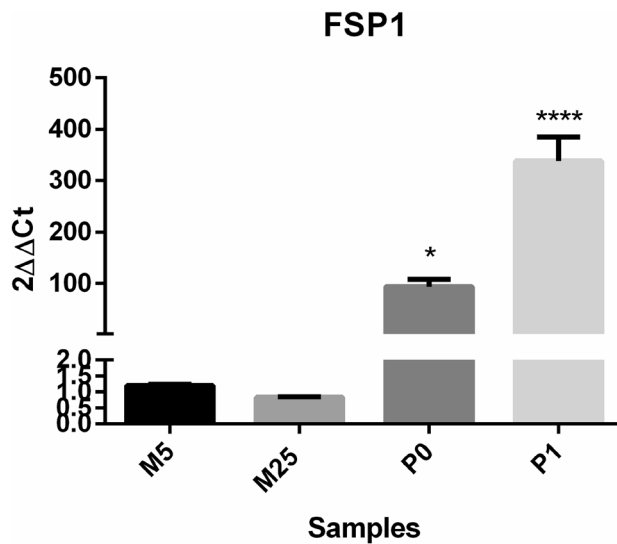


Figure 3. Fibroblast primary cultures exhibited significantly higher levels of FSP1 expression in comparison with canine mammary cancer cells (M5 and M25). M5 and M25 were used as reference samples to 2^{ΔΔCt} analysis. The 18S gene was used as the housekeeping gene (**p* < 0.05; *****p* < 0.0001; one way ANOVA followed by Tukey’s multiple comparison test).

monocultures in both CDMEM-F12 and CCM, while differences between cell-to-cell and transwell conditions were only observed from 144 h onwards (Fig. 7A). In monocultures, the use of CCM led to a significantly longer mast cell viability when compared to mast cells supplemented with CDMEM-F12, while no significant changes were observed between CCM and transwell conditions at any time-point. Finally, mast cells in monoculture

Ensemble ID	Gene name	LogFC	FDR
ENSCAFG00000017550	FSP1 (S100A4)	- 3.3209	2.03E-31
ENSCAF00000010387	FAP	- 8.1810	5.71E-18

Table 2. FSP1 and FAP mRNA levels measured by RNA-seq analysis.

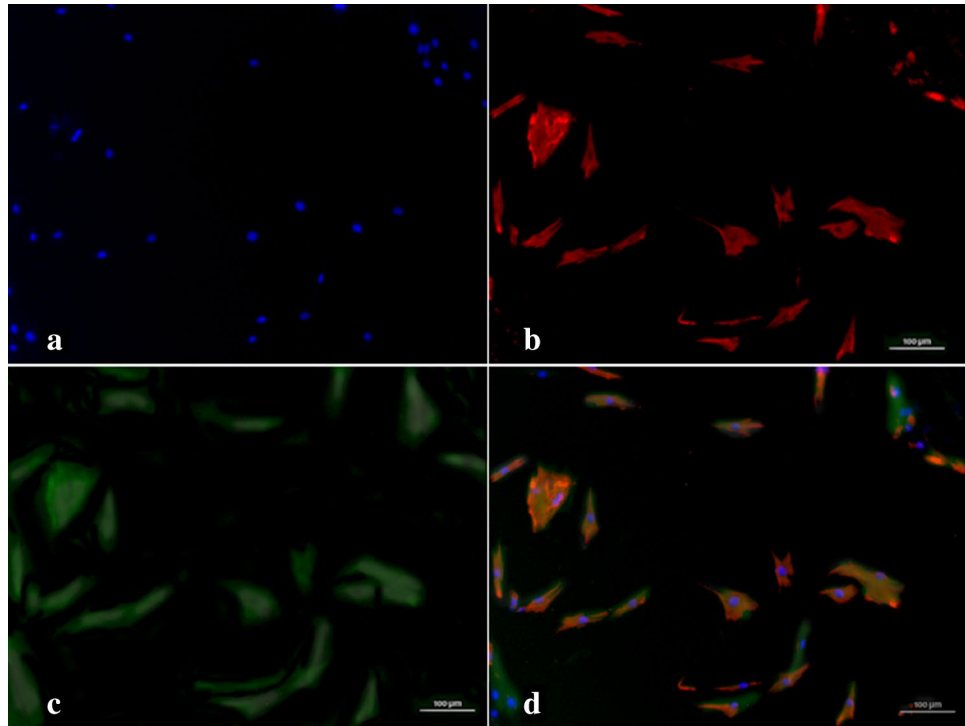


Figure 4. Representative immunofluorescence images of myofibroblasts from canine MCT culture. (a) Nuclei were stained with DAPI (4',6-diamidino-2-phenylindole dihydrochloride; blue). (b) Adherent cells in MCT culture stained with vimentin antibody (red) and (c) anti- α smooth muscle actin (α -SMA) antibody (Phalloidin-FITC, green). (d) The merged image shows overlapping expression (original magnification $\times 400$).

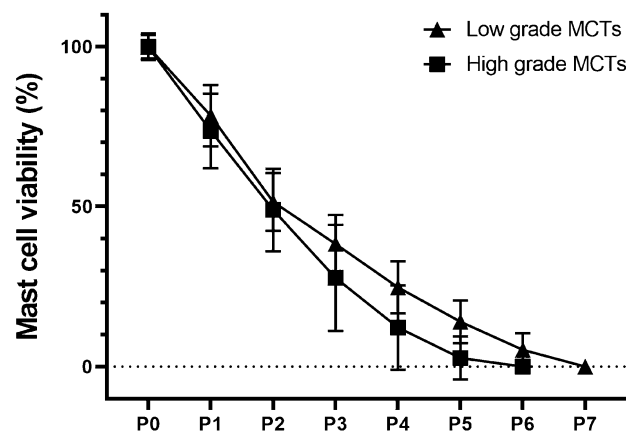


Figure 5. MCTs classified as low- and high-grade cultures at different passages along 11 weeks. Neoplastic mast cell culture (conditioned by fibroblasts) viability *versus* passages—percentage of viable mast cells during the passages of thirteen independent cultures from individual lesions. Samples are specified in Supplementary Table S1. Viability was determined by the Trypan blue exclusion method. Mean and Standard Deviation are represented in the graph, and no difference between low- and high-grade cultures were observed in any passage.

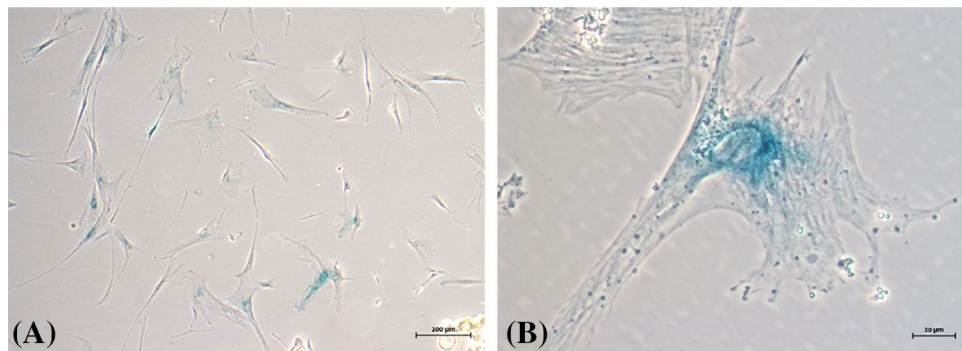


Figure 6. Cytochemical detection of Senescence-Associated β -Galactosidase (SA- β -Gal) activity in stromal fibroblasts of canine MCTs (Sample H05-16). Cells maintained in culture for 2 months (P5). **(A)** Positivity in most cells through the formation of blue precipitate in the cytoplasm. Bright field microscopy. **(B)** Fibroblasts demonstrating the most intense staining perinuclear. Phase contrast microscopy.

without any physical or chemical influence of adhered fibroblasts presented the lowest viability of all conditions, in which approximately 90% of cells died after 96 h of cultivation (Fig. 7B).

To investigate the possibility of neoplastic mast cells *in vitro* behaviour to be depended of histopathological grade, we compared low-grade and high-grade tumours in all four culture conditions. Differences between the two groups were found in all selected time-points in mast cells monoculture supplemented with CCM, where cells originated from low-grade samples presented a lower viability than those isolated from high-grade tumours (Fig. 8). The same pattern was found in the transwell system assay, although the significant difference was observed only after 192 h of cultivation. No differences were found in cell-to-cell contact and CDMEM-F12 monoculture conditions.

Discussion

In the present study, we demonstrated the inability of canine neoplastic mast cells to remain viable for long periods *in vitro* without the addition of growth factors or *in vivo* passages in mice, corroborating the observations of Pinello et al.³¹. The mast cells adhered to the fibroblasts but did not grow. The main reports on the establishment of cell lines from canine MCTs in continuous culture and with no previous passage in mice are: HRMC³², CM-MC, VI-MC, CoMS^{33,34}, MPT-1³⁵, MPT-1.2 cells³⁶ and MPT-2³⁷. However, in these studies, important characteristics were not described in detail, such as the number of passages with viable cells, the culture purification methods, culture conditions, and presence of fibroblasts or other cells in coculture. So far, long-term cultures of canine cutaneous mast cells are only possible with combined *in vitro* and *in vivo* approaches^{8–12}.

The notion that the mast cell phenotype can be importantly regulated by the microenvironment has been the subject of much discussion and interest. There are many possible factors that might have an effect on mast cell phenotype and influence mast cell *in vitro* survival^{37–39}, but CAFs are one of the most important components of the tumour microenvironment⁴¹. This feature has also been observed in human and murine mast cell lines^{42,43} and can be induced by cell-to-cell aggregation and mechanical handling effects⁵. In this study, neoplastic mast cells grew in suspension as single cells or in clusters, and this condition was similar to that observed in other canine MCT cultures^{33,35,45}.

In vivo, fibroblasts from cancer stroma undergo a myofibroblast transformation as part of the cellular response to neoplastic growth⁴⁵. MCT-derived CAFs are fundamental regulators of *in vitro* tumour maintenance and recognized essentially, but not exclusively, based on α -SMA expression^{46,47}. We confirmed the presence of myofibroblasts in canine MCT cultures in agreement with our previous findings in tumour tissue²⁹ and the observations of Giuliano et al.²⁸, which had identified CAFs in histopathological samples of canine MCTs. Fibroblast-secreted protein-1 (FSP1) produced by CAFs is another important factor in promoting the cancer cell growth that may have helped mast cell *in vitro* viability.

Knowing that neoplastic mast cell survival *in vitro* depends, in part, on the interaction with adhered cells, we employed different culture systems to elucidate the type of signalling. The mechanism of interaction across the cytoplasmic membrane should be considered, since mast cells form robust adhesions with fibroblasts in the coculture conditions⁴⁸ that are not mediated by known integrin or cadherin receptors⁴⁹. Notably, mast cells in monoculture normally grow in suspension and do not strongly adhere to plastic culture surfaces⁵⁰. Therefore, we considered that mast cell attachment to fibroblasts with intercellular signals may be important for *in vitro* mast cell short-term maintenance. We also believe that this cellular communication occurs through heterogeneous gap junction channels between neoplastic mast cells and CAFs^{51–54} promoting enhanced interleukin release⁴⁸.

Upon activation, CAFs secrete a vast repertoire of growth factors, such as hepatocyte (HGF), epidermal (EGF), insulin-like (IGF) growth factors and cytokines, including CXCL12 and IL-6⁵⁵. It was reported that IL-6 expression by CAFs is up to 100-fold higher than normal fibroblasts⁵⁶. Highlighting the importance of physical interaction between cells, fibroblasts are capable of producing IL-6 when stimulated directly by mast cell via cell-to-cell interaction in coculture^{57–59}, and less efficiently by mast cell mediators⁶⁰. IL-6 derived from CAFs and NCAFs is responsible for suppressing apoptosis in human intestinal mast cells⁶⁰ and hepatic mast cells⁶¹ under

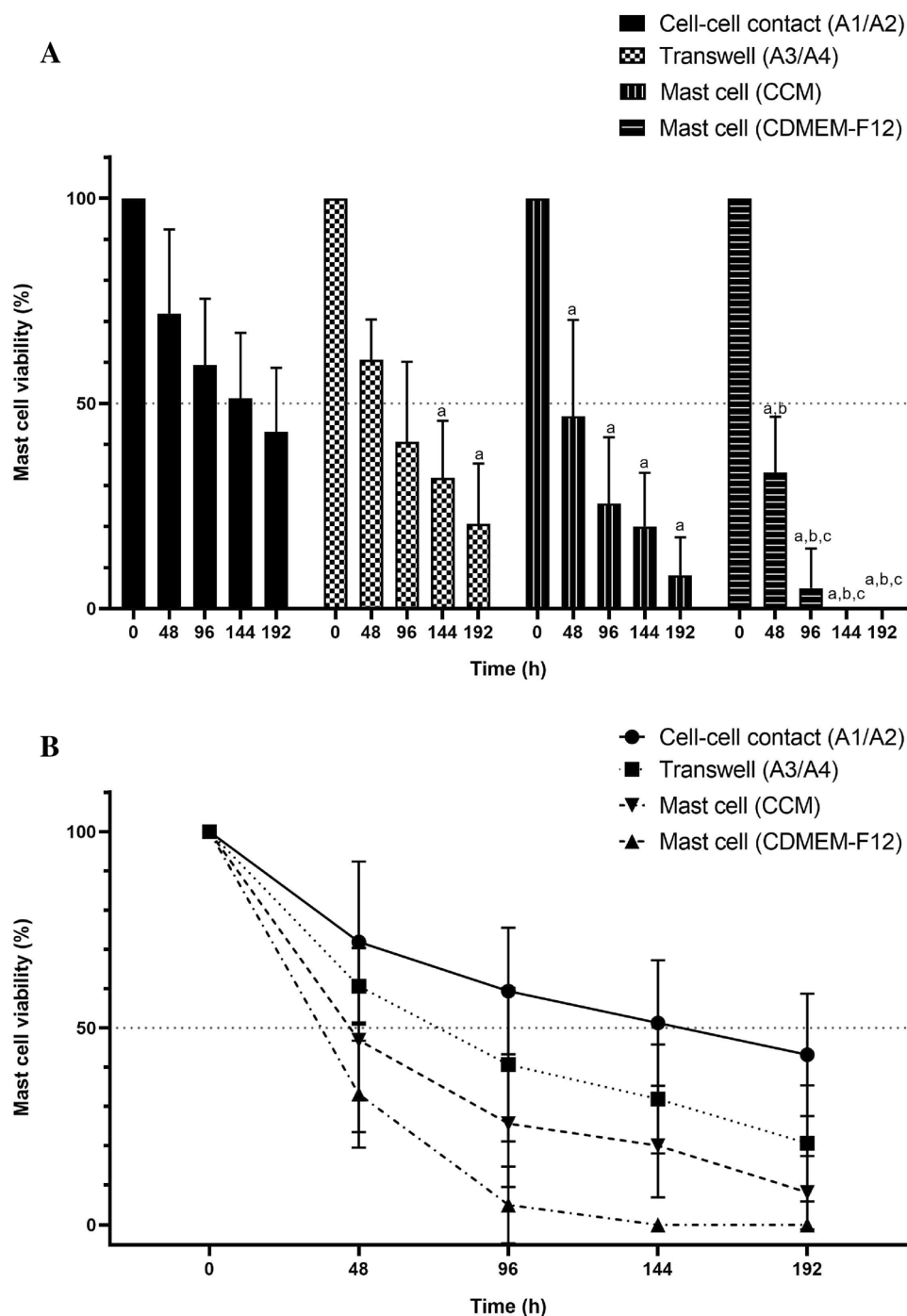


Figure 7. Results of the co-culture assay in four MCT samples (H550-17, H401-18, H1171-18 and H1249-18). **(A)** Each bar represents the mean and standard deviation of duplicate measurements. Canine mast cells cultured in cell-to-cell contact with an adherent layer of stromal fibroblasts showed the highest average number of viable cells in each time-point (a = $P < 0.05$ compared with cell–cell contact condition; b = $P < 0.05$ compared with Transwell co-culture system; c = $P < 0.05$ compared with mast cell in monoculture with CCM). **(B)** Tumour mast cell viability in each condition along 192 h of cultivation.

cell-to-cell contact condition. When bone marrow derived mast cells were cultured with a fibroblast monolayer, the IL-6 family of cytokines (IL-6, IL-11, OSM and LIF) induced proliferation of mast cells, but only when the fibroblasts were present. Thus, given that neoplastic mast cells and adherent cells were physically separated, it is likely that paracrine signalling through the pores of the membrane may be influencing mast cell population.

We also found that monocultures of canine neoplastic mast cells are not viable for more than four days in the absence of fibroblasts or their soluble factors. Similar results were obtained in vitro for mast cells cultured

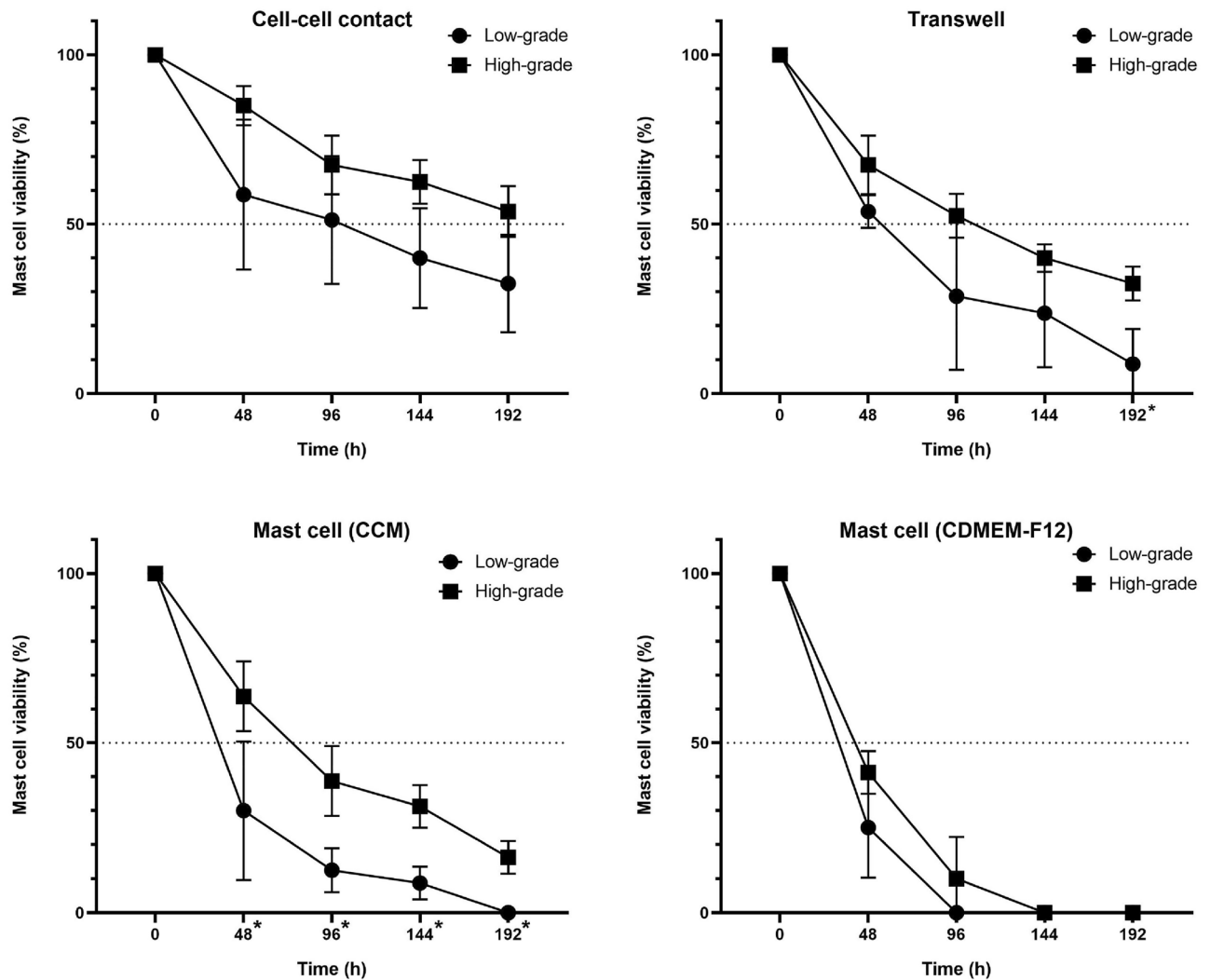


Figure 8. Comparison of neoplastic mast cells survival from low- and high-grade MCTs in each co-culture condition. Graphs show median \pm SD of mast cells viability up to 192 h. Statistical significance (*) was observed only in the transwell assay after 192 h (q value = 0.019) and in cultures supplied with complete cultured medium (CCM) after 48 (q value = 0.0268), 96 (q value = 0.007), 144 (q value = 0.0026) and 192 h (q value = 0.002).

without a stromal adherent cell layer^{16,31,39,43,62}. Interestingly, we did not detect differences between the two culture conditions with mast cells receiving conditioned medium (CCM), i.e., transwell assay and mast cells in monoculture with conditioned medium obtained from primary MCTs cultures supernatants. However, both conditions supported a superior number of viable mast cells compared to CDMEM-F12. We could attribute this finding to paracrine signalling between fibroblasts and mast cells.

The main limitations of the present study were the lack of knowledge about the exact composition of the conditioned medium and effective molecules secreted by the stromal fibroblasts in coculture. We believe that neoplastic mast cell survival *in vitro* depends, in part, on the interaction with the adhered fibroblasts and CAFs. Fibroblasts are known to secrete Stem Cell Factor (SCF), which is the main growth factor for mast cells^{38,40} and an essential factor for mast cell growth in rodent and human mast cells cultures^{38,62–64}. In addition, several studies with mast cell cultures indicated the requirement of both IL-3 and SCF to expansion and maturation, even in the presence of stromal cells^{62,65}. Literature data suggest that the establishment of mast cell lines in permanent culture *in vitro* with no passages by nude mice should depend on SCF supplemented medium^{40,64} and the presence of stromal cells may assist in the maintenance of mast cells *in vitro*^{14,17,62}. Finally, we need to consider that the partial decrease of mast cells in passages may in part reflect cell loss during the harvesting procedure⁵ or a relatively low density of the cultures.

The skin tumours used in this study provided a fibroblast population that declines *in vitro* with serial passaging, with increasing number of cells entering replicative senescence^{66–68}. We believe that the earlier onset of cell culture senescence may be due to the age of the cell culture donors^{67,69,70}. This process is thought to be caused by aging and these “aged” skin fibroblasts with limited replicative potential may be due to canine cellular aging *in vivo*, since the mean age of the dogs included in the present study was around 7.5 years.

We have also shown the presence of myofibroblasts in canine MCT cultures. This finding is in concordance with the observations of Giuliano et al.²⁸, which demonstrated that fibroblasts from canine MCT stroma have CAF phenotype and was correlated positively with high grade, high mitotic index and high Ki67 expression. We believe that this feature might be important to the understanding of the different clinical responses to chemotherapy, since CAFs could influence the drug-sensitivity of cancer cells⁷¹. Here, we have also shown that histopathological grade, which is related to the degree of cell differentiation, might have influenced survival in monocultures supplemented with CCM: mast cell viability was slightly higher in high-grade MCT-derived cultures. Although preliminary, due to the low number of samples, these results are interesting in the light of the different experimental approaches in literature, and could help to explain, for example, the higher invasion and metastatic rates in these cases, since neoplastic mast cells could be less dependent on cell-to-cell contact with fibroblasts. To the best of our knowledge, no previously published work compares the *in vitro* behaviour of tumours with different histopathological grades. Variability in mast cell phenotype as, for example, differences in the content of cellular proteases, reflects the action of the local microenvironment⁴⁰. The mechanisms underlying the relationship between the grade of malignancy and the culture conditions remain unclear and deserve future investigation.

Conclusion

In conclusion, reproducible development of canine tumour-derived mast cells by a long-term culture may need *in vivo* passages, fibroblasts interactions and/or supplemented medium with growth factors. Cultures without artificial stimuli would be a major breakthrough to understand canine MCT biology. Here, we showed that stromal MCT fibroblasts present a CAF phenotype *in vitro* when cocultured with neoplastic mast cells, constituting a promising and versatile *in vitro* model to study various aspects of MCTs. Fibroblasts and CAFs transcription factors could be important for MCT malignant phenotypes, through direct or indirect stimuli, in which different stroma cells cultured together communicate to create a tumour-permissive microenvironment and thus may contribute to the maintenance of cancer mast cells. Signalling mechanisms involved in these interactions are attractive therapeutic targets to block canine MCT progression. Ongoing studies in our laboratory aim to investigate canine mast cells and tumoral stroma cells interactions.

Materials and methods

Tumour samples. Mast cell tumour samples were obtained from dogs that underwent surgery at the Veterinary Hospitals of the Faculty of Animal Science and Food Engineering of the University of São Paulo (FZEA-USP) and the Octávio Bastos Foundation University (UNIFEOP), and private veterinary clinics, which agreed to participate in the present study. All surgical procedures were performed as part of the treatment, aiming the cure. Inclusion criteria were confirmed histopathological diagnosis of cutaneous MCT, no previous anti-neoplastic treatment (radio or chemotherapy) and availability of complete medical records. All experiments were approved by and performed in accordance with the guidelines and regulations of the Ethic Committee on Animal Use of the Faculty of Veterinary Medicine and Animal Science (protocol #CEUA/5637040718). The reporting in the manuscript follows the recommendations in the ARRIVE guidelines. Informed written consent was obtained from the owner of each dog whose MCT biopsy was included in this study. Patient treatment was unaffected by the study. All samples had a representative fragment placed in 10% neutral buffered formalin, processed routinely and embedded in paraffin. Four- μ m sections were stained with haematoxylin and eosin and MCTs were graded according to Kiupel et al.³⁰.

Dissociation and primary cell co-culture. Canine MCT samples obtained immediately after excisional biopsy under sterile conditions were placed in sterile transport medium at 4 °C consisting of Dulbecco's Modified Eagle Medium/Nutrient Mixture F-12 (DMEM-F12, Thermo Fisher, Fremont, California, USA), antibiotics penicillin G/streptomycin (200 U/mL, Sigma-Aldrich and 100 U/mL; Sigma-Aldrich, respectively) and 15% fetal bovine serum (FBS) until arrival at the laboratory. Subcutaneous fat tissue was removed and the tumours were minced finely into approximately 0.5–1.0 mm³ fragments and incubated in DMEM-F12 with an enzyme mixture: 200 U/mL collagenase type I (Sigma-Aldrich, St. Louis, MO, USA) and 100 U/mL hyaluronidase (Sigma-Aldrich, St. Louis, MO, USA) supplemented with 15% FBS and 2% antibiotics penicillin/streptomycin. After 180 min in water bath at 37 °C, the disaggregated tumour was filtered through a 100- μ m filter followed by filtration through a 40- μ m mesh (Cell Strainer, BD Biosciences). Cells dispersed by this procedure were centrifuged at 1500 rpm for 5 min at 25 °C and the sediment was re-suspended in DMEM-F12 supplemented with 15% of FBS and 1% of penicillin/streptomycin, denominated in this study as CDMEM-F12 for experimental purposes.

The cells obtained from the MCT were maintained at 37 °C in a 5% CO₂ atmosphere in two 75 mm² tissue culture flasks/sample with 10 mL of complete medium DMEM-F12. The medium was renewed every 5–7 days, when adherent cells reached confluence of approximately 70%. The supernatant with nonadherent cells was removed, centrifuged at 1500 rpm for 5 min, resuspended in complete DMEM-F12 medium and then passed to a sterile culture bottle flask with adherent cells at a density of 10⁵ cells per mL. The coculture was evaluated daily by Eclipse-TS100 microscope equipped with a Nikon camera (Nikon, Tokyo, Japan).

At each passage, a supernatant aliquot of 100 μ L was harvested, centrifuged at 1500 rpm for 5 min and the pellet placed on a glass slide. Mast cells were identified by 0.05% toluidine blue (Sigma-Aldrich Corp.) stain and with Romanowsky stain (Diff-Quik solution, Dade Behring Inc., Düdingen, Switzerland). Cell number was assessed in a Neubauer haemocytometer and cell viability was checked with Trypan Blue Exclusion Test according to Strober⁷², using an optical microscope (Eclipse TS100, Nikon, Japan).

Quantitative real-time polymerase chain reaction analysis for Fibroblast-specific Protein 1 (FSP 1). Total RNA was extracted from adherent cells derived from cultured canine cutaneous MCT at the initial (P0) and first passage (P1) using TRIzol reagent (Thermo) according to the manufacturer's instructions. NanoDrop2000 (Thermo Scientific, USA) and RNA integrity number (RIN) were used to verify the amount and integrity of the extracted RNA following manufacturer's protocol (RNA 6000 Nano kit, 2100 Bioanalyzer, Agilent Technologies, USA). Samples with A260/A280 ratio between 1.8 and 2.1 and RIN superior than 8 were considered appropriate for use. Subsequently, reverse transcription into cDNA was made using the commercial kit "High-Capacity cDNA Reverse Transcription Kit" (Thermo) at 37 °C for 120 min and 75 °C for 5 min in a PCR thermal cycler. Specific primers for Fibroblast-specific Protein 1 (FSP1) gene were designed with Primer-BLAST⁷³.

Real-time quantitative polymerase chain reaction (qRT-PCR) was performed with Fast SYBR Green Master Mix in a final volume of 10 μ L in the presence of primers for canine FSP1 gene: 5'-TCCTCATCTCTTCTCCTTCTTGGT-3' (forward) and 5'-TGAACCTTGTCACCCTCCTTGC-3' (reverse) in a final concentration of 50 nM. Primers were design with Primer-Blast⁷³ and the possibility of dimers and hairpins were verified using AutoDimer software⁷⁴. Primers were also analysed by in silico PCR to confirm specificity (<https://genome.ucsc.edu/cgi-bin/hgPcr>). Gene expression analysis were performed by qRT-PCR using a StepOne System (Thermo Fisher Scientific). Conditions for qPCR were as follows: 95 °C for 20 s; 40 cycles at 95 °C for 3 s for denaturation, 60 °C for 30 s for anneal/extend; melt curve analysis was performed at 95 °C for 15 s and 60 °C for 60 s. Relative expression levels of the target gene were normalized to the housekeeping gene (18S ribosomal RNA) and determined using the $2^{-\Delta\Delta C_t}$ method⁷⁵. The experiment was performed twice and in biological triplicates.

RNA-seq and differential expression. RNA libraries were constructed using the TruSeq Stranded mRNA LT Sample Prep Protocol and sequenced on Illumina HiSeq. 2500 equipment in a HiSeq Flow Cell v4 using HiSeq SBS Kit v4 (2 \times 100 pb). Sequencing quality was evaluated using the software FastQC (<http://www.bioinformatics.babraham.ac.uk/projects/fastqc>) and no additional filter was performed. Sequence alignment against the canine reference genome (CanFam3.1) was performed using STAR⁷⁶, according to the standard parameters and including the annotation file (Ensembl release 89). Secondary alignments, duplicated reads and reads failing vendor quality checks were removed using Samtools⁷⁷. Alignment quality was confirmed using Qualimap⁷⁸. Gene expression was estimated by read counts using HTseq⁷⁹ and normalized as counts per million reads (CPM). Only genes presenting at least 1 CPM were kept for differential expression (DE) analysis. Groups were divided between canine cancer cells (M5 and M25) and Fibroblasts (H250, H346, H395, H401, H402, and H1171). DE between the groups was performed using EdgeR package⁸⁰ on R environment, based on negative binomial distribution. Benjamini–Hochberg procedure was used to control the false discovery rate (FDR) and transcripts presenting FDR \leq 0.01 and log-Fold Change (logFC) > 1 or < -1 were considered differential expressed (DE).

In vitro characterization of adherent cells: immunofluorescence for α -smooth muscle actin (α -SMA) and vimentin. Fibroblasts derived from the MCT stroma were grown on glass coverslips right after tumour dissociation (P0) in complete DMEM F12 medium. Adherent cells were washed three times with PBS and then fixed in 4% paraformaldehyde solution (in PBS) for 10 min at room temperature. After washing with PBS, unspecific antigens were blocked for 45 min with a 5% fat-free skim milk solution at room temperature. Coverslips containing fixed cells were first incubated at 4 °C in humid chamber with the primary anti-vimentin antibody conjugated to fluorophore Alexa Fluor 647 (clone V9, cod. ab195878, Abcam, USA) diluted 1:100, for 16 h (overnight), washed and incubated for 60 min in a 1:500 dilution of monoclonal anti-alpha smooth muscle actin antibody conjugated to fluorescein isocyanate (FITC) (clone 1A4, Sigma-Aldrich, St Louis, MO, USA) at room temperature. After rinsing in PBS, nuclei were stained with DAPI. For the negative control, the antibodies were replaced with PBS. Coverslips were mounted on glass slides using ProLong solution (Thermo Scientific, USA) and observed immediately with an inverted fluorescence microscope (ZEISS—Axio Vert.A1) and photographed with a coupled camera AxioCam 503 attached using 540 nm wavelength filter for the observation of smooth muscle actin filaments (FITC) and 670–695 wavelength filter for visualization of vimentin (Alexa Fluor 647) and 358 nm for observation of the DAPI-labelled nuclei. Photomicrographs were taken using a ZEISS ZEN 2 Microscope Software (Carl Zeiss, Jena, Germany). All double immunofluorescence results were verified by single labelling techniques using direct (vimentin and alpha-actinin) fluorescence.

Adherent cells senescence assay. To assess cellular senescence in cultured fibroblast-like cells presenting a rapid decreasing in growth rate, we measured endogenous β -galactosidase activity as previously reported⁸¹. Fibroblasts used in this experiment were between passages 5 and 7. Briefly, cells were washed in PBS, fixed in 4% paraformaldehyde solution for 5 min at room temperature and incubated overnight at 37 °C with X-gal chromogenic substrate at pH 6.0 following the conventional protocol for SA- β -gal staining. The proportion of cells positive for β -gal activity can be easily determined by counting the number of blue cells in the total population. The cytochemical staining in senescent fibroblasts-like cells were observed by inverted ZEISS Axio Vert.A1 microscope and photographed with a coupled camera Axio Cam 503.

Co-culture transwell assay. Initially, cell populations obtained from primary tumours were cultivated in contact for 5–7 days. For each lesion, we obtained two bottles of primary culture at P0: one provided the neoplastic mast cells (supernatant) and CAFs (adhered); the other was maintained for supplying the tumour tissue culture medium (TTCM). Tumour cells cultured in P1 were used to perform the coculture transwell assay. Mast cells were obtained from the supernatant of primary cultures and CAFs adhered to the bottom were detached

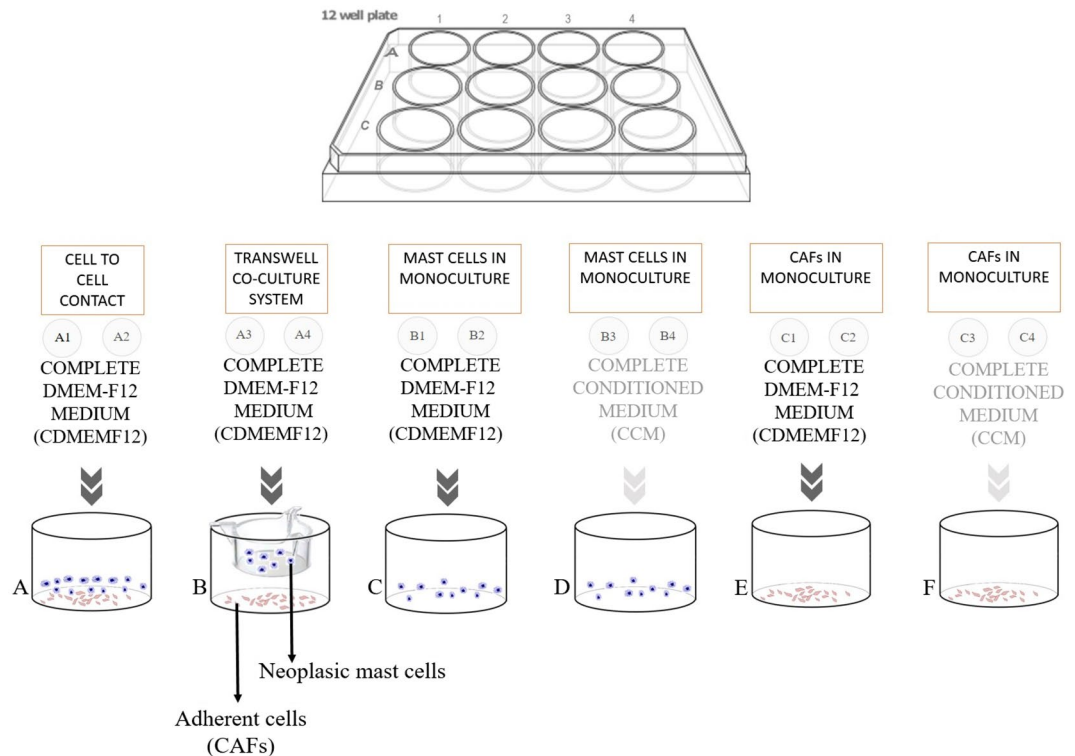


Figure 9. Coculture schematic model for the evaluation of neoplastic mast cells and stromal fibroblasts interactions. (A) Cell-to-cell coculture condition that allows the chemical and physical interaction between neoplastic mast cells and fibroblasts. (B) Transwell coculture system, with neoplastic mast cells and stromal fibroblasts in a condition that allows only chemical communication. Mast cells were added into the insert and fibroblasts into the well for adherence to the surface. (C) Mast cells in monoculture with complete DMEM-F12 medium and (D) with complete conditioned medium. (E) Fibroblasts in monoculture with complete DMEM-F12 medium and (F) with complete conditioned medium.

with enzymatic dissociation for 4–6 min at 37 °C in Trypsin (TrypLE Express 1X, with phenol red, Thermo Fisher Scientific). Two different media were used: complete DMEM-F12 medium (CDMEM-F12) when both cell types were present in the same well and complete conditioned medium (CCM) in monoculture wells, that was composed by one part of complete DMEM-F12 10× concentrated and nine parts of TTCM.

All assays were performed in duplicate, using a 12-well plate/tumour. Some wells received cell culture inserts with translucent polyester membrane (ThinCert, Greiner Bio-One, Kremsmünster, Austria). Pore sizes and density of the membrane were 0.4 µm and 2×10^6 pores/cm², respectively. In each well, 1×10^5 neoplastic mast cells were seeded. CAFs were seeded at an initial density of 1×10^4 cells/mL in a total medium volume of 1 mL/well.

The experiments were conducted under the following conditions: (1) Cell-to-cell contact, with mast cells seeded in direct contact with fibroblasts in a complete DMEM-F12 medium (CDMEM-F12) (Fig. 9A); (2) Transwell coculture system using cell culture inserts (ThinCert, Greiner Bio-One), in which two cell populations were placed in different compartments, i.e., neoplastic mast cells in the upper compartment (insert) and fibroblasts in the lower compartment (adhered to plate surface), in CDMEM-F12 medium (Fig. 9B); (3) Mast cells in monoculture, with neoplastic mast cells cultured alone in suspension receiving CDMEM-F12 medium (Fig. 9C) or CCM (Fig. 9D); and (4) Fibroblasts in monoculture maintained with CDMEM-F12 medium (Fig. 9E) or with CCM (Fig. 9F). Cocultures were maintained for 8 days at 37 °C and 5% CO₂, with daily observation using an inverted microscope (ZEISS Axio Vert.A1, Germany). Mast cell viability was determined by the Trypan blue exclusion method every 48 h with the removal of 10 µL supernatant of each insert/well with previous agitation. Cell counts and viability were examined at days 2, 4, 6 and 8. Adhered cells were not quantitatively evaluated (wells: C1, C2, C3 and C4). The experiment was maintained until death of all mast cells from some of the culture conditions.

Statistical analysis. The number of non-adherent mast cells obtained in the primary co-culture assay were presented as the mean ± standard deviation (SD) for each sample. Normality was tested using the Kolmogorov–Smirnov method. Comparison of mast cell viability for high- and low-grade cultures conditioned by fibroblasts and between co-culture conditions was performed using multiple t-tests, corrected for multiple comparisons using the Holm–Sidak method (alpha = 0.05). Comparison of mast cells viability in the co-culture assay considering each condition were performed with a 2-way ANOVA test, followed by correction for multiple comparisons using Tukey’s statistical hypothesis testing. Significance level was defined as 0.05 (95% confidence interval). All statistical analyses were conducted using GraphPad Prism (GraphPad Software, CA, USA).

Data availability

The datasets generated during and/or analyzed during the current study are available from the corresponding author on reasonable request.

Received: 4 June 2021; Accepted: 5 October 2021

Published online: 13 December 2021

References

- Galli, S. J. The mast cell: A versatile effector cell for a challenging world. *Int. Arch. Allergy Immunol.* **113**, 14–22 (1997).
- Blackwood, L. *et al.* European consensus document on mast cell tumours in dogs and cats. *Vet. Comp. Oncol.* **10**, e1–e29. <https://doi.org/10.1111/j.1476-5829.2012.00341.x> (2012).
- Soll, A. H., Lewin, K. & Beaven, M. A. Isolation of histamine-containing cells from canine fundic mucosa. *Gastroenterol.* **77**, 1283–1290 (1979).
- Soll, A. H., Toomey, M., Culp, D., Shanahan, F. & Beaven, M. A. Modulation of histamine release from canine fundic mucosal mast cells. *Am. J. Physiol. Gastrointest. Liver Physiol.* **254**, G40–G48 (1988).
- Demora, F., Garcia, G., Puigdemont, A., Arboix, M. & Ferrer, L. Skin mast cell releasability in dogs with atopic dermatitis. *Inflamm. Res.* **45**, 424–427 (1996).
- Brazis, P., Queralt, M., de Mora, F., Ferrer, L. I. & Puigdemont, A. Stem cell factor enhances IgE-mediated histamine and TNF-alpha release from dispersed canine cutaneous mast cells. *Vet. Immunol. Immunopathol.* **75**, 97–108 (2000).
- Lin, T. Y., Rush, L. J. & London, C. A. Generation and characterization of bone marrow-derived cultured canine mast cells. *Vet. Immunol. Immunopathol.* **113**, 37–52 (2006).
- Lazarus, S. C. *et al.* Isolated canine mastocytoma cells: Propagation and characterization of two cell lines. *Am. J. Phys. Cell Physiol.* **251**, C935–C944 (1986).
- Caughey, G. H., Lazarus, S. C., Viro, N. F., Gold, W. M. & Nadel, J. A. Tryptase and chymase: comparison of extraction and release in two dog mastocytoma lines. *Immunol.* **63**, 339 (1988).
- Devinney, R. & Gold, W. M. Establishment of two dog mastocytoma cell lines in continuous culture. *Studies* **9**, 10 (1990).
- Nagamine, M. K. *et al.* In vitro inhibitory effect of trichostatin A on canine grade 3 mast cell tumor. *Vet. Res. Comm.* **35**, 391–399 (2011).
- Ishiguro, T. *et al.* Establishment and characterization of a new canine mast cell tumor cell line. *J. Vet. Med. Sci.* **63**, 1031–1034 (2001).
- Akula, S. *et al.* How relevant are bone marrow-derived mast cells (BMMCs) as models for tissue mast cells? A comparative transcriptome analysis of BMMCs and peritoneal mast cells. *Cells* **9**, 2118. <https://doi.org/10.3390/cells9092118> (2020).
- Levi-Schaffer, F., Austen, K. F., Gravallesse, P. M. & Stevens, R. L. Coculture of interleukin 3-dependent mouse mast cells with fibroblasts results in a phenotypic change of the mast cells. *Proc. Natl. Acad. Sci.* **83**, 6485–6488 (1986).
- Rennick, D., Hunte, B., Holland, G. & Thompson-Snipes, L. Cofactors are essential for stem cell factor-dependent growth and maturation of mast cell progenitors: Comparative effects of interleukin-3 (IL-3), IL-4, IL-10, and fibroblasts. *Blood* **85**, 57–65 (1995).
- Marquis, B. J. & Haynes, C. L. The effects of co-culture of fibroblasts on mast cell exocytotic release characteristics as evaluated by carbon-fiber microelectrode amperometry. *Biophys. Chem.* **137**, 63–69 (2008).
- Raizman, M. B., Austen, K. F. & Katz, H. R. Mast cell heterogeneity. Differential synthesis and expression of glycosphingolipids by mouse serosal mast cells as compared to IL-3-dependent bone marrow culture-derived mast cells before or after coculture with 3T3 fibroblasts. *J. Immunol.* **145**, 1463–1468 (1990).
- Nabeshima, Y. *et al.* IL-4 modulates the histamine content of mast cells in a mast cell/fibroblast co-culture through a Stat6 signaling pathway in fibroblasts. *FEBS Lett.* **579**, 6653–6658 (2005).
- Walker, M. A., Harley, R. A. & Leroy, E. C. Inhibition of fibrosis in TSK mice by blocking mast cell degranulation. *J. Rheumatol.* **14**, 299–301 (1987).
- Gruber, B. L. Mast cells: Accessory cells which potentiate fibrosis. *Int. Rev. Immunol.* **12**, 259–279 (1995).
- Gruber, B. L. *et al.* Human mast cells activate fibroblasts: Tryptase is a fibrogenic factor stimulating collagen messenger ribonucleic acid synthesis and fibroblast chemotaxis. *J. Immunol.* **158**, 2310–2317 (1997).
- Ito, A., Nakajima, S., Sasaguri, Y., Nagase, H. & Mori, Y. Co-culture of human breast adenocarcinoma MCF-7 cells and human dermal fibroblasts enhances the production of matrix metalloproteinases 1, 2 and 3 in fibroblasts. *Br. J. Cancer* **71**, 1039 (1995).
- Qian, L. W. *et al.* Co-cultivation of pancreatic cancer cells with orthotopic tumor-derived fibroblasts: Fibroblasts stimulate tumor cell invasion via HGF secretion whereas cancer cells exert a minor regulative effect on fibroblasts HGF production. *Cancer Lett.* **190**, 105–112 (2003).
- Suzuki, S., Sato, M., Senoo, H. & Ishikawa, K. Direct cell–cell interaction enhances pro-MMP-2 production and activation in co-culture of laryngeal cancer cells and fibroblasts: involvement of EMMPRIN and MT1-MMP. *Exp. Cell Res.* **293**, 259–266 (2004).
- Samoszuk, M., Tan, J. & Chorn, G. Clonogenic growth of human breast cancer cells co-cultured in direct contact with serum-activated fibroblasts. *Breast Cancer Res.* **7**, R274 (2005).
- Hwang, R. F. *et al.* Cancer-associated stromal fibroblasts promote pancreatic tumor progression. *Cancer Res.* **68**, 918–926 (2008).
- Wei, L. Y. *et al.* Reciprocal activation of cancer-associated fibroblasts and oral squamous carcinoma cells through CXCL1. *Oral Oncol.* **88**, 115–123 (2019).
- Giuliano, A., Dos Santos Horta, R., Constantino-Casas, F., Hoather, T. & Dobson, J. Expression of fibroblast activating protein and correlation with histological grade, mitotic index and Ki67 expression in canine mast cell tumours. *J. Comput. Pathol.* **156**, 14–20 (2017).
- Pulz, L. H. *et al.* Identification of two molecular subtypes in canine mast cell tumours through gene expression profiling. *PLoS One* **14**, e0217343. <https://doi.org/10.1371/journal.pone.0217343> (2019).
- Kiupel, M. *et al.* Proposal of a 2-tier histologic grading system for canine cutaneous mast cell tumors to more accurately predict biological behavior. *Vet. Pathol.* **48**, 147–155 (2011).
- Pinello, K. C. *et al.* In vitro chemosensitivity of canine mast cell tumors grades II and III to all-trans-retinoic acid (ATRA). *Vet. Res. Commun.* **33**, 581–588 (2009).
- Ohmori, K. *et al.* Identification of c-kit mutations-independent neoplastic cell proliferation of canine mast cells. *Vet. Immunol. Immunopathol.* **126**, 43–53 (2008).
- Takahashi, T. *et al.* IgG-mediated histamine release from canine mastocytoma-derived cells. *Int. Arch. Allergy Immunol.* **125**, 228–235 (2001).
- Takahashi, T. *et al.* Role of $\beta 1$ integrins in adhesion of canine mastocytoma cells to extracellular matrix proteins. *J. Vet. Med. Sci.* **69**, 495–499 (2007).
- Amagai, Y., Tanaka, A., Ohmori, K. & Matsuda, H. Establishment of a novel high-affinity IgE receptor-positive canine mast cell line with wild-type c-kit receptors. *Biochem. Biophys. Res. Commun.* **366**, 857–861 (2008).

36. Amagai, Y. *et al.* The phosphoinositide 3-kinase pathway is crucial for the growth of canine mast cell tumors. *J. Vet. Med. Sci.* **75**, 791–794 (2013).
37. Matsuda, A. *et al.* Glucocorticoid sensitivity depends on expression levels of glucocorticoid receptors in canine neoplastic mast cells. *Vet. Immunol. Immunopathol.* **144**, 321–328 (2011).
38. Dvorak, A. M., Furitsu, T., Kissell-Rainville, S. & Ishizaka, T. Ultrastructural identification of human mast cells resembling skin mast cells stimulated to develop in long-term human cord blood mononuclear cells cultured with 3T3 murine skin fibroblasts. *J. Leuk. Biol.* **51**, 557–569 (1992).
39. Dvorak, A. M., Schleimer, R. P., Schulman, E. S. & Lichtenstein, L. M. Human mast cells use conservation and condensation mechanisms during recovery from degranulation. In vitro studies with mast cells purified from human lungs. *Lab. Invest.* **54**, 663–678 (1986).
40. Rossi, G. L., di Comite, V. & Olivieri, D. Mast cell cultures: Bench to bedside. *Clin. Exp. Allergy* **28**, 1182–1190 (1998).
41. Xing, F., Saidou, J. & Watabe, K. Cancer associated fibroblasts (CAFs) in tumor microenvironment. *Front. Biosci.* **15**, 166–179 (2010).
42. Tertian, G., Yung, Y.-P., Guy-Grand, D. & Moore, M. A. Long-term in vitro culture of murine mast cells. I. Description of a growth factor-dependent culture technique. *J. Immunol.* **127**, 788–794 (1981).
43. Horton, M. A. & O'Brien, H. A. Characterization of human mast cells in long-term culture. *Blood* **62**, 1251–1260 (1983).
44. Garcia, G. *et al.* Comparative morphofunctional study of dispersed mature canine cutaneous mast cells and BR cells, a poorly differentiated mast cell line from a dog subcutaneous mastocytoma. *Vet. Immunol. Immunopathol.* **62**, 323–337 (1998).
45. Chiavegato, A., Bochaton-Piallat, M. L., D'Amore, E., Sartore, S. & Gabbiani, G. Expression of myosin heavy chain isoforms in mammary epithelial cells and in myofibroblasts from different fibrotic settings during neoplasia. *Virchows Arch.* **426**, 77–86 (1995).
46. Valenti, M. T. *et al.* Conditioned medium from MCF-7 cell line induces myofibroblast differentiation, decreased cell proliferation, and increased apoptosis in cultured normal fibroblasts but not in fibroblasts from malignant breast tissue. *Histochem. J.* **33**, 499–509 (2001).
47. Kojima, Y. *et al.* Autocrine TGF- β and stromal cell-derived factor-1 (SDF-1) signaling drives the evolution of tumor-promoting mammary stromal myofibroblasts. *Proc. Natl. Acad. Sci.* **107**, 20009–20014 (2010).
48. Termei, R., Laschinger, C., Lee, W. & McCulloch, C. A. Intercellular interactions between mast cells and fibroblasts promote pro-inflammatory signaling. *Exp. Cell Res.* **319**, 1839–1851 (2013).
49. Trautmann, A., Feunerstein, B., Ernst, N., Bröcker, E. B. & Klein, C. E. Heterotypic cell–cell adhesion of human mast cells to fibroblasts. *Arch. Dermatol. Res.* **289**, 194–203 (1997).
50. Baggolini, M., Walz, A. & Kunkel, S. L. Neutrophil-activating peptide-1/interleukin 8, a novel cytokine that activates neutrophils. *J. Clin. Invest.* **84**, 1045–1049 (1989).
51. Salomon, D., Saurat, J. H. & Meda, P. Cell-to-cell communication within intact human skin. *J. Clin. Invest.* **82**, 248–254 (1988).
52. Moyer, K. E., Siggers, G. C. & Ehrlich, H. P. Mast cells promote fibroblast populated collagen lattice contraction through gap junction intercellular communication. *Wound Repair Regen.* **12**, 269–275 (2004).
53. Au, S. R., Au, K., Siggers, G. C., Karne, N. & Ehrlich, H. P. Rat mast cells communicate with fibroblasts via gap junction intercellular communications. *J. Cell. Biochem.* **100**, 1170–1177 (2007).
54. Foley, T. T. & Ehrlich, H. P. Through gap junction communications, cocultured mast cells and fibroblasts generate fibroblast activities allied with hypertrophic scarring. *Plastic Reconstr. Surg.* **131**, 1036–1044 (2013).
55. Santi, A., Kugeratski, F. G. & Zanivan, S. Cancer associated fibroblasts: The architects of stroma remodeling. *Proteomics* **18**, 1700167 (2018).
56. Hugo, H. J. *et al.* Contribution of fibroblast and mast cell (afferent) and tumor (efferent) IL-6 effects within the tumor microenvironment. *Cancer Microenviron.* **5**, 83–93 (2012).
57. Trautmann, A., Krohne, G., Bröcker, E. B. & Klein, C. E. Human mast cells augment fibroblast proliferation by heterotypic cell–cell adhesion and action of IL-4. *J. Immunol.* **160**, 5053–5057 (1998).
58. Gyotoku, E. *et al.* The IL-6 family cytokines, interleukin-6, interleukin-11, oncostatin M, and leukemia inhibitory factor, enhance mast cell growth through fibroblast-dependent pathway in mice. *Arch. Dermatol. Res.* **293**, 508–514 (2001).
59. Fitzgerald, S. M., Lee, S. A., Hall, H. K., Chi, D. S. & Krishnaswamy, G. Human lung fibroblasts express interleukin-6 in response to signaling after mast cell contact. *Am. J. Resp. Cell Mol. Biol.* **30**, 585–593 (2004).
60. Montier, Y. *et al.* Central role of IL-6 and MMP-1 for cross talk between human intestinal mast cells and human intestinal fibroblasts. *Immunobiol.* **217**, 912–919 (2012).
61. Kambe, M., Kambe, N., Oskeritzian, C. A., Schechter, N. & Schwartz, L. B. IL-6 attenuates apoptosis, while neither IL-6 nor IL-10 affect the numbers or protease phenotype of fetal liver-derived human mast cells. *Clin. Exp. Allergy* **31**, 1077–1085 (2001).
62. Yamada, N., Matsushima, H., Tagaya, Y., Shimada, S. & Katz, S. I. Generation of a large number of connective tissue type mast cells by culture of murine fetal skin cells. *J. Invest. Dermatol.* **121**, 1425–1432 (2003).
63. Tsai, M. *et al.* Induction of mast cell proliferation, maturation, and heparin synthesis by the rat c-kit ligand, stem cell factor. *Proc. Natl. Acad. Sci.* **88**, 6382–6386 (1991).
64. Lee, H. N., Kim, C. H., Song, G. G. & Cho, S. W. Effects of IL-3 and SCF on histamine production kinetics and cell phenotype in rat bone marrow-derived mast cells. *Immune Netw.* **10**, 15–25 (2010).
65. Ogawa, M. *et al.* Suspension culture of human mast cells/basophils from umbilical cord blood mononuclear cells. *Proc. Natl. Acad. Sci.* **80**, 4494–4498 (1983).
66. Martin, G. M., Sprague, C. A. & Epstein, C. J. Replicative life-span of cultivated human cells. *Lab. Invest.* **23**, 86–92 (1970).
67. Schneider, E. L. & Mitsui, Y. The relationship between in vitro cellular aging and in vivo human age. *Proc. Natl. Acad. Sci.* **73**, 3584–3588 (1976).
68. Funk, W. D. *et al.* Telomerase expression restores dermal integrity to in vitro-aged fibroblasts in a reconstituted skin model. *Exp. Cell Res.* **258**, 270–278 (2000).
69. Bowman, P. D., Meek, R. L. & Daniel, C. W. Aging of human fibroblasts in vitro: correlations between DNA synthetic ability and cell size. *Exp. Cell Res.* **93**, 184–190 (1975).
70. Kohn, R. R. Aging and cell division. *Science* **188**, 203–204 (1975).
71. Östman, A. & Augsten, M. Cancer-associated fibroblasts and tumor growth—bystanders turning into key players. *Curr. Opin. Gen. Dev.* **19**, 67–73 (2009).
72. Strober, W. Trypan blue exclusion test of cell viability. *Curr. Protoc. Immunol.* **21**, A.3B.1–A.3B.2 (1997).
73. Ye, J. *et al.* Primer-BLAST: A tool to design target-specific primers for polymerase chain reaction. *BMC Bioinform.* **13**, 134 (2012).
74. Vallone, P. M. & Butler, J. M. AutoDimer: A screening tool for primer-dimer and hairpin structures. *Biotechniques* **37**, 226–231 (2004).
75. Livak, K. J. & Schmittgen, T. D. Analysis of relative gene expression data using real-time quantitative PCR and the 2^{- $\Delta\Delta$ CT} method. *Methods* **25**, 402–408 (2001).
76. Dobin, A. *et al.* STAR: Ultrafast universal RNA-seq aligner. *Bioinformatics* **29**, 15–21 (2013).
77. Li, H. *et al.* The Sequence Alignment/Map format and SAMtools. *Bioinformatics* **25**, 2078–2079 (2009).
78. Garcia-Alcalde, F. *et al.* Qualimap: Evaluating next-generation sequencing alignment data. *Bioinformatics* **28**, 2678–2679 (2012).
79. Anders, S. *et al.* HTSeq—A Python framework to work with high-throughput sequencing data. *Bioinformatics* **31**, 166–169 (2015).

80. Robinson, M. D. *et al.* edgeR: A Bioconductor package for differential expression analysis of digital gene expression data. *Bioinformatics* **26**, 139–140 (2010).
81. Dimri, G. P. *et al.* A biomarker that identifies senescent human cells in culture and in aging skin in vivo. *Proc. Natl. Acad. Sci.* **92**, 9363–9367 (1995).

Acknowledgements

The authors would like to thank Nilton P. dos Santos and Lindsay B. Paskoski for technical support, and the veterinarians who submitted surgical specimens for this study. This research was funded by Fundação de Amparo à Pesquisa do Estado de São Paulo (FAPESP), Grants #2016/03862-1 and #2021/11567-8, Coordenação de Aperfeiçoamento de Pessoal de Nível Superior (CAPES) and Conselho Nacional de Desenvolvimento Científico e Tecnológico (CNPq).

Author contributions

Conceptualization, L.H.P, H.F. and R.F.S.; formal analysis, L.H.P., Y.G.C., P.L.P.X., H.F. and R.F.S.; data curation, L.H.P., G.C.H., K.G.C., A.L.R., A.T.N., S.H.F., P.L.P.X.; writing—original draft preparation, L.H.P.; writing—review and editing, Y.G.C., G.C.H., K.G.C., A.L.R., P.L.P.X., A.T.N., S.H.F., H.F. and R.F.S; project administration and funding acquisition, R.F.S. All authors have read and agreed to the published version of the manuscript.

Funding

Coordenação de Aperfeiçoamento de Pessoal de Nível Superior, Conselho Nacional de Desenvolvimento Científico e Tecnológico, Fundação de Amparo à Pesquisa do Estado de São Paulo (Grants No. 2016/03862-1 and #2021/11567-8).

Competing interests

The authors declare no competing interests.

Additional information

Supplementary Information The online version contains supplementary material available at <https://doi.org/10.1038/s41598-021-03390-w>.

Correspondence and requests for materials should be addressed to R.F.S.

Reprints and permissions information is available at www.nature.com/reprints.

Publisher's note Springer Nature remains neutral with regard to jurisdictional claims in published maps and institutional affiliations.



Open Access This article is licensed under a Creative Commons Attribution 4.0 International License, which permits use, sharing, adaptation, distribution and reproduction in any medium or format, as long as you give appropriate credit to the original author(s) and the source, provide a link to the Creative Commons licence, and indicate if changes were made. The images or other third party material in this article are included in the article's Creative Commons licence, unless indicated otherwise in a credit line to the material. If material is not included in the article's Creative Commons licence and your intended use is not permitted by statutory regulation or exceeds the permitted use, you will need to obtain permission directly from the copyright holder. To view a copy of this licence, visit <http://creativecommons.org/licenses/by/4.0/>.

© The Author(s) 2021